ISBN: 978-3-95450-255-4 ISSN: 2226-0358 doi: 10.18429/JACoW-ICALEPCS2025-TUPD094

NANOSCALE PRECISION MULTI-AXIS MOTION CONTROL FOR THE CBXFEL PROJECT*

M.A. Montironi†,[1], W. Lewis[2], S.J. Stein[2], N. Balakrishnan[1], T. Thayer[1], X. Permanyer[1],
M. Balcazar[1], D. Zhu[1], A. Halavanau[1], A. Lutman[1], H.-D. Nuhn[1],
Z. Huang[1], Y. Shvyd'ko[3], R. Lindberg[3], D. Shu[3], M. White[3], G. Lanza[1]
[1]SLAC National Accelerator Laboratory, Menlo Park, CA, USA
[2]Osprey DCS, MD, USA
[3]Argonne National Laboratory, Lemont, IL, USA

Abstract

The Cavity-Based Free Electron Laser (CBXFEL) project is proposing to produce a recirculating X-ray cavity and deploy it to the SLAC LCLS (Linac Coherent Light Source) Hard X-ray (HXR) undulator line. The shape of the cavity is defined by four diamond crystals which must be positioned with nanometer-level accuracy in four Degrees-Of-Freedom (DOF). Additionally, several electron and X-ray beam diagnostic components need to be precisely positioned to achieve, monitor, and maintain the cavity alignment. These functions are accomplished by a total of sixty-nine motion axes, eight of which are actuated by lead-screw stages operated by stepper motors, thirty-seven by Ultra High Vacuum (UHV) SmarAct piezo stages, and twenty-four by custom designed flexure stages actuated by UHV piezo linear actuators. The flexure stages are driven by UHV piezo actuators and real-time position feedback is provided by capacitive sensors and optical interferometers. A motion control system based on the CK3M PMAC architecture was developed to drive the different motion stages. This paper describes the main requirements to be met, how the technologies were integrated into the accelerator control system, and the main lessons learned.

INTRODUCTION

The Cavity-Based Free Electron Laser (CBXFEL) project is proposing to produce a recirculating X-ray cavity and deploy it to the SLAC LCLS (Linac Coherent Light Source) Hard X-ray (HXR) undulator line [1, 2]. Figure 1 shows the experimental layout where the optical cavity, defined by four Bragg-reflecting crystal mirrors (C1, C2, C3, C4), encloses the first seven HXR undulator segments. Dipole magnets in a chicane configuration divert the incoming electron beam around C4 and re-insert it in the first undulator segment to generate x-rays. Another chicane diverts the electron beam exiting the seventh undulator segment, around C1, and re-inserts it in the eighth undulator segment just downstream of C1.

Beyond the C1-C4 crystals, the CBXFEL system is composed of several in-vacuum and in-air beam diagnostics and movers organized in six stations: A, B, C, D, E, and F as shown in Fig. 1. Design for an additional station, G, planned for the experimental hutches, will be finalized once Station B installation is completed.

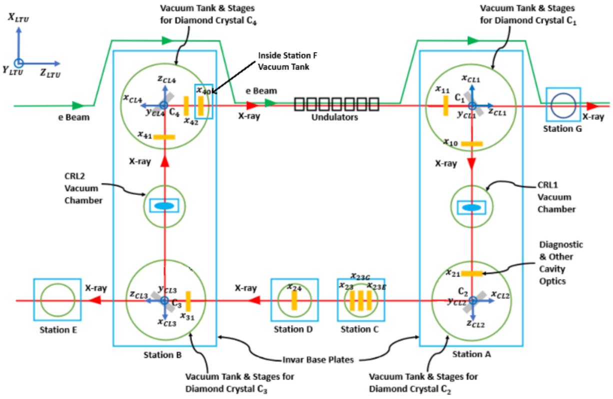

Figure 1: CBXFEL experimental layout.

Station A

Station A, located in HXR cell 21, hosts the C1 and C2 diamond crystals, three X-ray Beam Position/Profile Monitors (X11, X10, and X21), and one Compound Reflective Lens (CRL1)

Station B

Station B, located in HXR cell 13, hosts the C3 and C4 diamond crystals, three X-ray Beam Position/Profile Monitors (X31, X41, and X42), and one Compound Reflective Lens (CRL2)

Station C

Station C, located along the return line, hosts three X-ray Beam Position and Profile Monitors (X23E, X23G, and X23) as well as a beam sampling diffraction grating.

Station D

Station D, located along the return line, hosts one X-ray Beam Profile Monitor (X24).

Station E

Station E, located along the return line, hosts a Beam Position/Profile monitor and two photodiodes.

Station F

Station F, located downstream of Station B in HXR cell 13, hosts a Beam Overlap Diagnostic (BOD).

---

* Work supported by US Department of Energy Office of Science Under Contracts DE-AC01-06CH11357 and DE-AC02-76FO0515

† alexmon@slac.stanford.edu

MOTION CONTROL ARCHITECTURE

The four diamond crystals and all the other beam diagnostic elements described in the previous section can be positioned in space to shape the X-ray cavity and to adjust the interaction point between the diagnostic elements and the X-ray beam path. Ultra-High Vacuum (UHV) compatible SmarAct [3] piezo stages are used to position the X11, X10, X21, CRL1, X31, X41, X42, CRL2, X23, X23G, X23E, and X24 diagnostic components as seen, for example, in Fig. 2. To achieve the positioning accuracy needed to position the four diamond crystals and shape the x-ray optical cavity (1000 µm range, 50 nm resolution for the linear stages, 15 mrad range, 20 nrad resolution for the angular stages), flexure stages based on the weak-link mechanism technique [4] were developed. Because of lower positioning accuracy requirements (100 mm travel range, 1 µm resolution), the station E detectors and station F BOD were designed to be actuated by stepper motors and commercially available lead-screw linear stages.

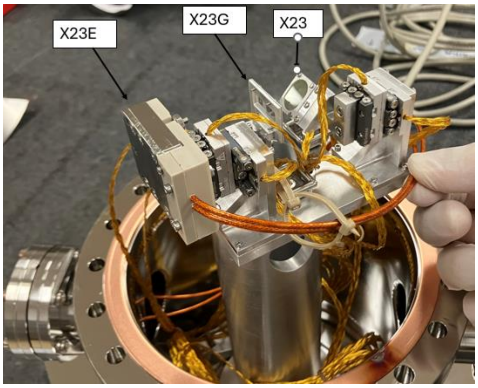

Figure 2: CBXFEL Station C diagnostic components and SmarAct piezo stages.

Diamond Crystal Positioning

Each diamond crystal shaping the CBXFEL optical cavity can be positioned in four degrees of freedom (two translations and two rotations) with sub-micron and sub-milliradian precision using in-vacuum flexure stages actuated by Ultra High Vacuum (UHV) compatible piezo linear actuators [5, 6] with position feedback provided by in-vacuum capacitive sensors and optical interferometers [7, 8]. The position of the roll and pitch flexure stages can be set using two different actuators: a coarse actuator whose feedback comes from the on-stage capacitive sensor and a fine actuator using as feedback the position of the end target calculated from two independent interferometer readings. The purpose of the roll and pitch fine actuators is to compensate angular crosstalk originating when the flexure stages in the stack are actuated. Each diamond crystal can also be inserted into the X-ray beam path and the interaction point adjusted by a stack of three UHV compatible SmarAct [3] stages (Dp, Ds, Dy) as shown in Fig. 3 and Fig. 4.

Before the CBXFEL project, no equivalent motion control applications had been deployed to the SLAC accelerator motion control system. Different motion control architectures were thus evaluated to select the most suitable in terms of flexibility, ability to handle complex kinematics, and reliability. The Omron Automation CK3M Programmable Multi-Axis Motion Controller (PMAC) [9] was selected for its proven motion control performance, its ability to interface with different feedback and actuator types, and established EPICS integration. The CK3M-based motion control architecture shown in Fig. 4 was then developed to control the C1-C4 diamond crystals.

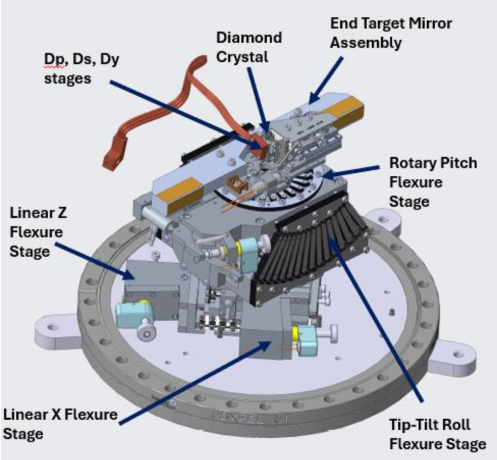

Figure 3: CAD view of C1 with motion stages and diamond crystal highlighted.

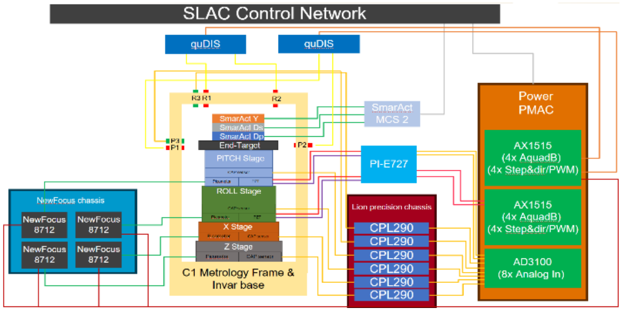

Figure 4: Schematic representation of the CBXFEL diamond crystal positioning stack motion control architecture.

Figure 5 shows the software configuration developed to allow the CK3M PMAC controlling each stage to interface with the six piezo actuators, the four on-stage capacitive sensors, the two end-target capacitive sensors, and the four end-target interferometers (Fig. 4). The Z, X, coarse roll, and coarse pitch actuators are controlled using Pulse-Frequency Modulated (PFM) signals and the PMAC was configured with two motor structures for each physical actuator. One motor structure, normally disabled, for open-loop PFM control, and one for closed-loop control. A PLC program reacting to user inputs allows switching between closed and open loop. A cascade control loop was implemented to interface with the fine roll and pitch actuators since they are controlled by a DC voltage that needs to be maintained constant to keep the actuator in position. Other PLC programs were implemented to kill a motor once the target position is reached and to dynamically set the soft

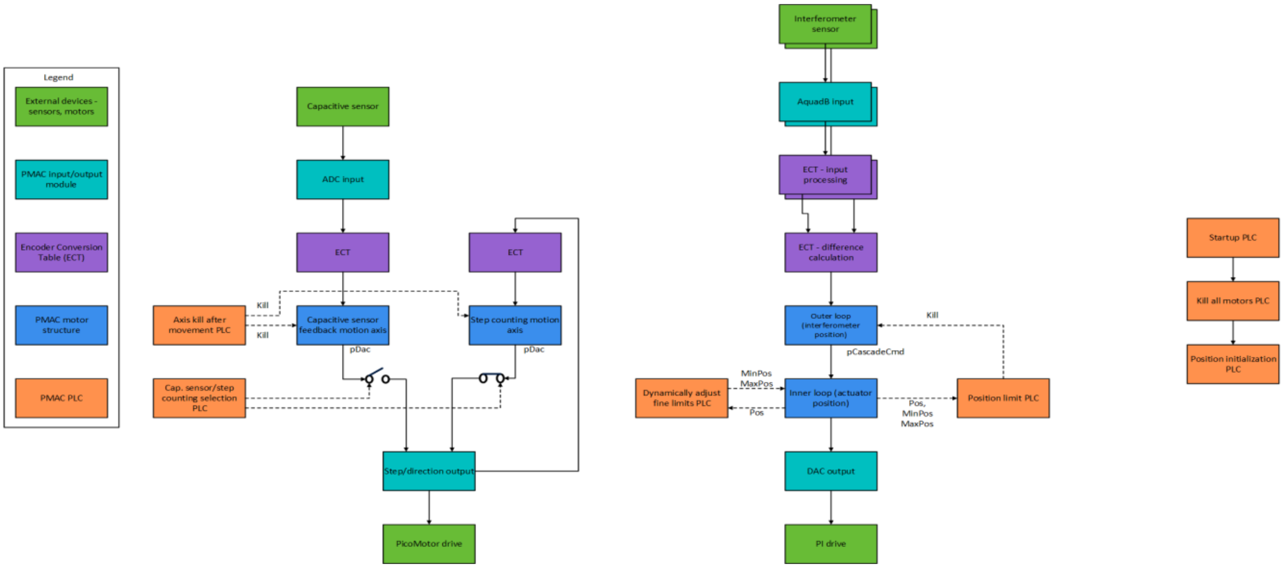

Figure 5: CBXFEL PMAC motion control software architecture.

limit of the fine actuators based on the coarse stage position.

The ability of the fine roll and pitch actuators to maintain the angular position of the end-target and thus of the diamond mirror was determined by performing scan tests. During such tests, one of the linear stages was repetitively moved through its motion range while the position of the end-target was monitored. Figure 6 shows the data collected during a scan of the Z axis with the fine roll motor disabled, thus not compensating for any angular crosstalk. Figure 7 shows the data collected with the fine roll motor compensating. The tests determined that crosstalk compensation can maintain the angle of the end-target, and thus of the diamond crystal, stable within +/- 0.0005 milliradians

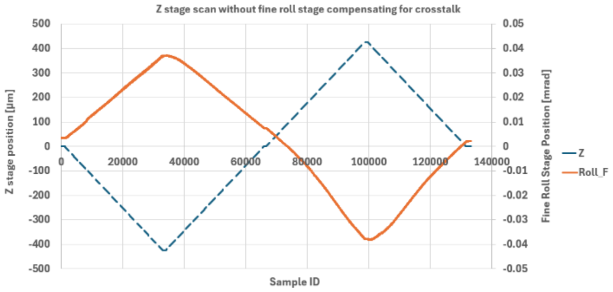

Figure 6: Z flexure stage scan with fine roll actuator not compensating angular crosstalk.

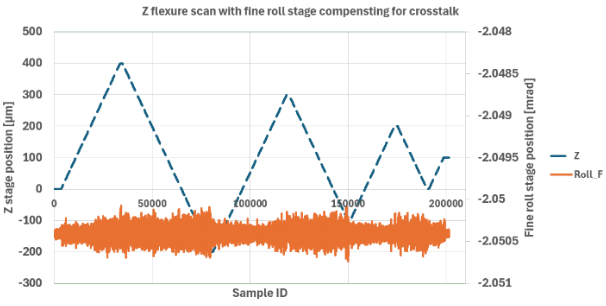

Figure 7: Z flexure stage scan with fine roll actuator compensating angular crosstalk.

Led Screw Actuated Linear Stages

Due to less stringent positioning requirements and larger design motion range, the actuation mechanism for the station E and F diagnostic devices is based on stepper motors, linear optical or magnetic encoders, and linear stages driven by lead screws. Six axes of motion are required for station E, a three DOF linear stage stack to position the beam diagnostics and a three DOF stage stack to position a camera. The beam diagnostics stages are controlled in closed loop using magnetic linear BiSS-C encoders while the camera stages are controlled in open loop. Two axes are required for station F, one to insert and retract the BOD and one to position a diagnostic camera, both operating in closed loop using optical linear BiSS-C encoders. A single eight-axis PMAC CK3M motor controller with serial encoder modules was selected for this application. The controller handles closed-loop motion control and open loop motion control. It also handles reaction to two motion limit switches for each axis, homing for the open loop stages, and fault detection from the stepper amplifiers and encoders. Figure 8 is a schematic representation of the Stations E and F motion control architecture.

EPICS Integration

All the PMAC and SmarAct motor controllers can interface with the EPICS-based accelerator control network over Ethernet/IP using drivers available from the community [10, 11]. The CBXFEL EPICS motion control interface was designed to be modular, and, except for a few exceptions, the IOCs are tied to individual vacuum chambers to simplify deployment and maintenance. The lower-level interface to each controllable axis is through a motor record instance and, in addition, a higher-level interface was created to allow users to save operationally relevant setpoints and directly drive the axes to those setpoints. Records and user interfaces to collect and display system status and faults were also created to simplify operation. The main CBXFEL motion control user interface, shown in Fig. 9, was designed to provide access to all relevant parameters including vacuum levels, Machine Protection System (MPS) status, IOC status, Asyn interfaces, and remotely operated Power Distribution Units (PDU) control.

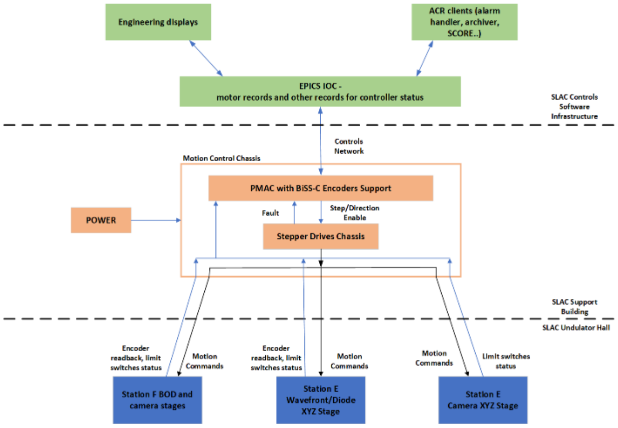

Figure 8: CBXFEL Station E and F motion control architecture.

INSTALLATION STATUS

Since all the actuators in Stations A, B, C, and D are piezo-based, limitations on the maximum length of the cables meant that all controls electronics and infrastructure had to be designed to be installed locally in the undulator hall. The motion control electronics for stations E and F were instead installed in the support buildings as the selected stepper actuators and linear encoders allow for longer cable runs. Three new racks were installed in HXR cell 13 to support the Station B motion control electronics and three in cell 21 to support Station A. Station C and D motion controllers were installed locally on specially designed fixtures anchored to the stations support stands. Figure 10 shows the station C fixture, the station E and F motion control rack in the support building, and one of the station A racks in the undulator hall. Given the large (42) number of new motor controllers and related electronics the CBXFEL project is planning to install in the SLAC undulator hall, the control system infrastructure designed and deployed for the LCLS-II project had to be expanded. New cable trays and long-haul cables were installed together with new network cables, patch panels and switches. A staged installation plan was devised to install components as they became available. Station E was the first to be installed in the Summer of 2024, followed by stations C, D, F, and finally C1 and CRL1 in the summer of 2025. C2 and Station B are planned to be installed in the Fall of 2025 and winter of 2026.

Figure 10: Clockwise from top left: station C fixture to hold the motor controller, station E and F motion control rack, and one of the C1 motion control racks.

CONCLUSION

The CBXFEL project introduced new advanced technologies to the LCLS accelerator motion control system. A new PMAC-based motion control architecture was designed, implemented, and deployed to interface with the diamond crystal nanopositioning stage stack. Mechanical installation is reaching the final stages, and most of the motion control systems have already been deployed. Physics commissioning started in early 2025 and is expected to continue throughout 2026.

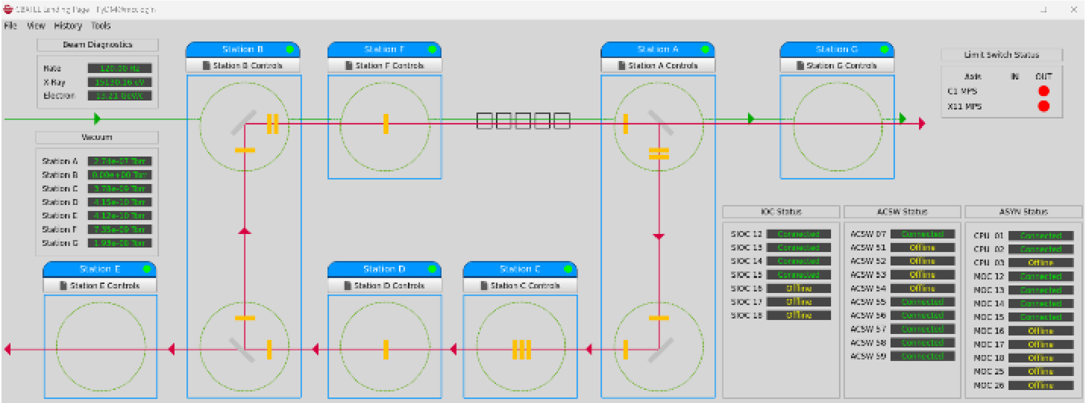

Beam Diagnostics

Rate 120.00 Hz
X-Ray 15130.36 eV
Electron 13.21 GeV

Vacuum

Station A 2.74e-07 Torr
Station B 0.00e+00 Torr
Station C 3.70e-09 Torr
Station D 4.15e-10 Torr
Station E 4.12e-10 Torr
Station F 7.35e-09 Torr
Station G 1.93e-08 Torr

IOC Status

SIOC 12 Connected
SIOC 13 Connected
SIOC 14 Connected
SIOC 15 Connected
SIOC 16 Offline
SIOC 17 Offline
SIOC 18 Offline

ACSW Status

ACSW 07 Connected
ACSW 51 Offline
ACSW 52 Offline
ACSW 53 Offline
ACSW 54 Offline
ACSW 55 Connected
ACSW 56 Connected
ACSW 57 Connected
ACSW 58 Connected
ACSW 59 Connected

ASYN Status

CPU 01 Connected
CPU 02 Connected
CPU 03 Offline
MOC 12 Connected
MOC 13 Connected
MOC 14 Connected
MOC 15 Connected
MOC 16 Offline
MOC 17 Offline
MOC 18 Offline
MOC 25 Offline
MOC 26 Offline

Figure 9: CBXFEL main motion control user interface.

REFERENCES

[1] M. White *et al.*, “CBXFEL design, production, and installation status,” in *Proc. LINAC'24*, Chicago, IL, USA, Aug. 2024, pp. 758-761. `doi:10.18429/JACoW-LINAC2024-THPB060`

[2] P. Liu *et al.*, “X-ray optics for the cavity-based X-ray free-electron laser,” *J. Synchrotron Radiat.*, vol. 31, no. 4, pp. 751–762, Jun. 2024. `doi:10.1107/s1600577524003977`

[3] SmarAct, SLC-17, `https://www.smaract.com/en/linear-stages/type/slc-17`

[4] D. Shu et al., “Design of the nanopositioning and mechanical system for cavity-based X-ray free electron laser,” *Journal of Physics: Conference Series*, vol. 2380, no. 1, p. 012029, Dec. 2022. `doi:10.1088/1742-6596/2380/1/012029`

[5] Picomotor Actuator, Ultra-High Vacuum, 0.5 in. Travel, 0.375 in., Shank Model: 8301-UHV, `https://www.newport.com/p/8301-UHV`

[6] P-841 Preloaded Piezo Actuators, `https://www.pi-usa.us/en/products/piezo-actuators-stacks-benders-tubes/p-841-preloaded-piezo-actuators-412418452`

[7] Lion Precision, Capacitive Sensors, `https://www.lionprecision.com/products/capacitive-sensors/.`

[8] qutools, quDIS Interferometric Displacement Measurement, `https://qutools.com/qudis/.`

[9] Omron, CK3M Programmable Multi-Axis Motion Controller, `https://automation.omron.com/en/us/products/family/CK3M`

[10] Github, Diamond Light Source, pmac, `https://github.com/DiamondLightSource/pmac/tree/dls-master`

[11] Github, epics-modules/motor, `https://github.com/epics-modules/motor`